Electrochromic devices based on in situ polymerised EDOT and Prussian Blue: influence of transparent conducting oxide and electrolyte composition-towards up-scaling

Sandrine Duluard, Ayse Celik-Cochet, Iyad Saadeddin, Anne Labouret, Guy Campet, Gerhard Schottner, Uwe Posset, Marie-Hélène Delville

Electrochromic devices based on *in situ* polymerised EDOT and Prussian Blue: influence of transparent conducting oxide and electrolyte composition—towards up-scaling†‡

Sandrine Duluard,[a] Ayse Celik-Cochet,[b] Iyad Saadeddin,[ac] Anne Labouret,[d] Guy Campet,[a] Gerhard Schottner,[b] Uwe Posset[b] and Marie-Helene Delville*[a]

DOI: 10.1039/c1nj20231f

Inorganic/organic (hybrid) complementary electrochromic devices (ECDs) of the type [transparent conducting oxide (TCO)//inorganic counter electrode/hydrophobic electrolytic membrane/polymeric working electrode//TCO] were assembled. The working electrodes consisted of spin-coated polymer films prepared by moderator-controlled *in situ* oxidative chemical polymerisation of 3,4-ethylene dioxythiophene (EDOT). Thin, galvanostatically deposited Prussian Blue (PB) films were employed as counter electrodes. Besides $F:SnO_2$ (FTO)/glass and $Sn:In_2O_3$ (ITO)/glass, a flexible ITO/PET film was alternatively used for materials deposition. In order to attain the maximum device performance, the PB charge capacity was monitored and adapted to the capacity of the EDOT polymer films. The two electrochromic electrodes were separated by a novel hydrophobic polymer electrolyte based on a gel of 1-butyl-3-methyl-imidazolium bis(trifluoromethanesulfonyl)imide (BMI-TFSI) and poly(methylmethacrylate) (PMMA), with lithium bis(trifluoromethanesulfonyl)imide (LiTFSI) as the salt. The influence of two parameters—ITO sheet resistance and the PMMA content in the electrolyte—on the final device properties was investigated. The ITO sheet resistance value proved to be crucial for the switching kinetics. The variation of the weight ratio of PMMA in the electrolyte showed that the effect on the kinetics is small whereas the change in absorbance is highly affected. The properties of the complementary glass-based devices were eventually compared to the corresponding plastic-based electrochromic elements. First attempts to scale up the technology were made for flexible 12×15 cm^2 (active area) devices.

Introduction

Since the discovery of inherently conductive polymers (ICPs) there has been huge interest in their use as organic conductors for a large variety of applications in particular electronic devices. ICPs gain electrical conductivity by oxidation or reduction, usually accompanied by the insertion of anionic or cationic species to ensure charge neutrality.[1] Most ICPs are potentially electrochromic and able to change their optical absorption characteristics depending on their redox state. They can thus be used in electrochromic devices (ECDs), *i.e.*, for smart windows with variable transmittance, high contrast displays, anti-dazzling rear view mirrors, and optical attenuators.[2–4] They have also been identified in other areas (coatings, electromagnetic shielding, artificial muscles, light-emitting diodes, field-effect transistors, photovoltaic cells and batteries,[5] actuators,[6] nanocontainers,[7] biomedical engineering.[8]

The major challenges for smart windows are to develop inexpensive devices exhibiting a reproducible optical response during repetitive cycling between bleached and darkened states, at the lowest possible cost and longest lifetime (ten years for windows). These systems should also be (i) low-energy consuming for both their manufacture and their operation, (ii) as light as possible (plastic substrates) and flexible.

In general, ECDs consist of two complementary electrochromic materials deposited on transparent current collectors, usually transparent conductive oxide substrates. An ion-conducting electrolyte is placed in between and separates both half-cells from each other.[9,10] Poly(3,4-ethylenedioxythiophene) (PEDOT),[11]

[a] *CNRS, Université de Bordeaux, ICMCB, 87 avenue Dr A. Schweitzer, Pessac, F-33608, France. E-mail: delville@icmcb-bordeaux.cnrs.fr; Fax: +33 540002761; Tel: +33 540008460*
[b] *Fraunhofer ISC, Neunerplatz 2, 97082 Wuerzburg, Germany. E-mail: uwe.posset@isc.fraunhofer.de*
[c] *College of Sciences, An-Najah National University, PO Box 7, Nablus, Palestine. E-mail: iyadl2002@yahoo.com*
[d] *Solems, 3 rue Léon Blum, 91120 Palaiseau, France. E-mail: anne.labouret@solems.com*

† Dedicated to Professor Didier Astruc for his 65th birthday.

‡ Electronic supplementary information (ESI) available: Transmittance of the flexible up-scaled device after 10, 450, and 21 000 cycles. See DOI: 10.1039/c1nj20231f

a well-known π-conjugated electrochromic polymer, shows a very high colouration efficiency as well as fairly high conductivity and transparency in its oxidised state.[12,13] It has therefore been suggested for many applications, such as medical biosensing,[14] and optoelectronic,[15] photovoltaic[16] or electrochromic devices.[12,17,18] PEDOT can be synthesised *via* electrochemical or oxidative chemical polymerisation of the monomer 3,4-ethylenedioxythiophene (EDOT). Electrochemical polymerisation may result in inhomogeneous films when large areas have to be coated, and the incorporation of any desired functional additives in the coatings is hardly possible. On the other hand, *in situ* chemical polymerisation has proven to be a viable technique for the coating of large ($>10 \times 10$ cm^2) area substrates, yielding well-defined ICP films with smooth surfaces and high electrochemical activity. Notwithstanding the large number of publications dealing with the chemical polymerisation of alkylene dioxythiophenes,[19–21] only a few authors mention the use of this method for the preparation of ECDs. The deposition of poly(alkylenedioxythiophenes) as thin films *via in situ* chemical oxidative polymerisation of a hydroxyl-functional derivative of EDOT (EDOT-MeOH)[22] for a use in electrolyte capacitors has, however, been described by Bayer Corporation.[23]

In this paper, the formation of thin PEDOT films *via in situ* chemical oxidative polymerisation is described and their performance in full ECDs is illustrated. Complementary ECDs of different configurations were assembled, *i.e.*, hybrid ITO/glass- (type A) and PET/ITO-based (type B) assemblies of inorganic counter electrodes and polymeric working electrodes. While ITO/glass of different sheet resistances ranging from 24 to 124 Ω sq^{-1} was employed, the ITO/PET film showed a sheet resistance of 60 Ω sq^{-1}.

The PEDOT films (working electrodes) were prepared by means of spin coating *via* moderator controlled *in situ* oxidative chemical polymerisation. Thin Prussian Blue (PB, $Fe^{III}_4(Fe^{II}(CN)_6]_3$) films (counter electrodes) were electrochemically deposited according to a procedure published earlier.[24,25] In order to achieve maximum electrochromic performance in the devices, the PB charge capacity was monitored and adapted to the charge capacity of the PEDOT films determined beforehand. Both so-called half-cells were assembled in their coloured states, separated by a hydrophobic polymer gel electrolyte membrane.[26] The latter consisted of the ionic liquid 1-butyl-3-methyl-imidazolium bis(trifluoromethanesulfonyl)imide (BMI-TFSI), the thickener poly(methylmethacrylate) (PMMA), and the salt lithium bis(trifluoromethanesulfonyl)imide (LiTFSI). The PMMA weight ratio was varied and resulted in gels of different viscosities. PMMA[27] was chosen for this purpose due to its high optical transparency[28,29] and durability. It also shows favourable adhesion properties when plasticised properly.[30]

Electrochemical and spectro-electrochemical techniques were employed to study the influence of ITO sheet resistance and polymer electrolyte composition on device performance, in particular on switching kinetics and long term cycling stability. Glass-based devices were compared to ECDs built up on a conducting plastic film showing intermediate ITO sheet resistance. Eventually, a scale-up of the device could be performed.

Experimental section

Preparation of PEDOT *via in situ* chemical polymerisation

An EDOT monomer (Baytron M from H. C. Starck) was chemically polymerised *in situ* (isp) on pre-cleaned transparent conductive oxide substrates according to a procedure described earlier by Y. Ha *et al.*[31] 0.625 mmol of the moderator base (imidazol, Aldrich) were dissolved in *n*-butanol (Aldrich) and kept in an ultrasonic bath until a clear solution was obtained. Afterwards, 2.5 mmol of EDOT and 4.38 mmol of oxidiser ($Fe(OTs)_3$, Aldrich) were added to the mixture in the given order. The solution was stirred for 5 min and then filtered through a 0.45 μm syringe membrane filter. Within a period of 10 min after the addition of the oxidiser, the coating solution was applied by means of a KSM Karl-Süss spin coater model RC8. 5×5 cm^2 sized ITO-glass panels with sheet resistances of 24, 58, and 124 Ω sq^{-1} (Solems) as well as 5×5 cm^2 sized pieces of the ITO-PET film with 60 Ω sq^{-1} (Bekaert) were used as substrates. The solution was spun off subsequently at 600 revolutions per minute (rpm) for 30 s and at 1200 rpm for 10 s. The wet films were then transferred to an oven where the polymerisation was completed at 120 °C for 20 min. After the thermal treatment, unreacted oxidiser and the monomer were removed by careful rinsing in *n*-butanol and drying with compressed air. This procedure yielded almost fully oxidised PEDOT films doped with tosylate ions.[32] The thickness of the coatings was determined by means of a reflectometer, model NanoCalc 2000-UV-VIS. Values in the range of 200–250 nm were typically obtained. The surface morphology and elemental composition of the deposits were investigated by means of a scanning electron microscope, model Hitachi S800, equipped for energy dispersive X-ray microanalysis (EDX), LEO model 1450 VP 133 with a Si(Li)-Detector system. Micro-Raman spectroscopy (Dilor, Model LABRAM, excitation wavelength: 632.8 nm) was used to obtain vibrational spectra. The electrochemical studies, except for spectro-electrochemical measurements, were performed in a glove box under an inert argon atmosphere using a Voltalab PGZ301 potentiostat. Volta-bsorptometry and spectro-electrochemical measurements were carried out in an electrochemical cell, placed in an Evolution 100 spectrometer (Thermo Electron Corporation). The working electrodes were either fluorine-doped tin oxide (FTO)/glass or PET/ITO, the auxiliary electrode was a platinum foil, and a Ag/AgCl wire was used as a pseudo-reference electrode. The latter was calibrated against a Saturated Calomel Electrode (SCE). Using this setup, charge capacities of around 1.5 mC cm^{-2} were determined for as-prepared PEDOT films.

Preparation of Prussian Blue films *via* electrodeposition

The electrodeposition of PB was performed according to a procedure described earlier.[24] The deposition was carried out in a three-electrode cell: platinum foil and a saturated calomel electrode were employed as counter and pseudo-reference electrodes, respectively. The substrates to be coated were placed as working electrodes. PB was deposited from a solution of 10^{-2} M $FeCl_3 \cdot 6H_2O$ (Aldrich, 98%) and 10^{-2} M $K_3[Fe(CN)_6]$ (Aldrich, 99%) in water. A reduction current density of -18 μA cm^{-2} was applied for 75 s in order to match

the capacity value of PEDOT as determined beforehand. The obtained PB films were dried at 70 °C for 2 h under vacuum.

ECD assembly and characterisation

Complementary inorganic/organic (hybrid) ECDs were assembled according to the following configurations: Device A: [*glass*/*ITO*//Prussian Blue/hydrophobic gel electrolyte/PEDOT//*ITO*/*glass*]; Device B: [*PET*/*ITO*//Prussian Blue/hydrophobic gel electrolyte/PEDOT//*ITO*/*PET*]. The half-cells were assembled in their coloured states, *i.e.* PB in its mixed valence state (Fe(III)–Fe(II)) and PEDOT in its reduced (*i.e.*, neutral) state. The oxidised PEDOT films obtained by *in situ* polymerisation (see above) hence had to be reduced, which was performed by applying a reducing potential of −1.0 V *vs.* Ag/AgCl in a three-electrode cell filled with an electrolyte solution of 0.1 M LiTFSI in BMI-TFSI.

A hydrophobic polymer gel electrolyte was prepared from a 0.03/0.97 mixture (molar ratio) of LiTFSI (Aldrich, >99.95%) and BMI-TFSI (Solvionic, 99%), to which a 30 wt% of PMMA (Aldrich, M_w = 96 400) was added. The mixture was diluted with butanone and deposited on the PB electrode by the doctor blade coating technique. After evaporation of the solvent, the reduced PEDOT film and the PB/polymer electrolyte combination were then assembled into a full device by pressing at 70 °C for 2 h under vacuum. The structure of the full device is depicted in Fig. 1. The PEDOT film was always taken as the working electrode while the PB layer was defined as a counter and reference (RE) electrode.

Spectro-electrochemical characterisation of the ECDs was performed by means of a spectrophotometer model Nicolet Evolution 100 ($1050 \leq \lambda \leq 350$ nm) for UV-Visible spectroscopy measurements and a potentiostat Voltalab 40 for electrical measurements. The samples to be studied were placed in the UV-Visible spectrophotometer and potentials were applied in a two-electrode configuration.

Results and discussion

Surface morphology and spectral analysis of PEDOT and PB individual films

The individual isp-PEDOT and PB films were rather smooth and homogenous with a low surface roughness (Fig. 2a: PEDOT, Fig. 2b: PB), proving that, *via* the chosen deposition techniques, thin highly transparent films without agglomerations can be obtained.

The SEM images show the films in their as-obtained states (no potential applied). The cracks on the films were made

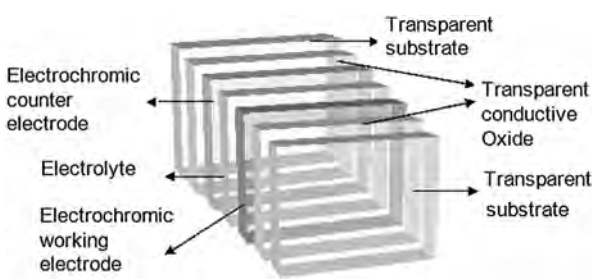

Fig. 1 Layers composing the electrochromic devices.

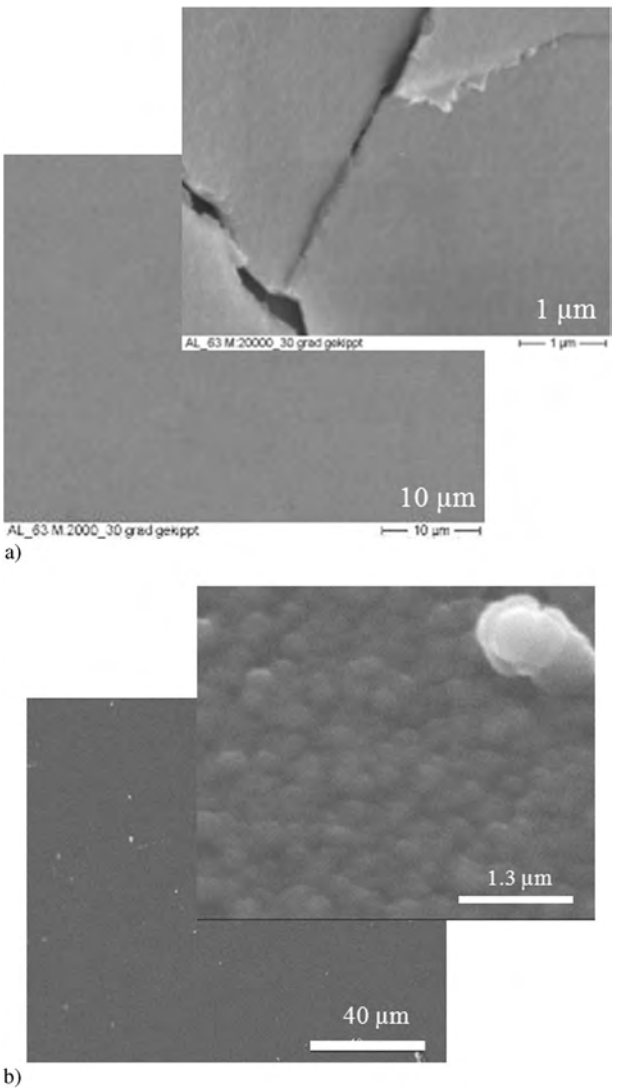

Fig. 2 SEM images of (a) isp-PEDOT and (b) PB films prepared on transparent conducting substrates.

on purpose to get an idea of the film thickness by SEM. The thickness of the PEDOT and PB films was estimated from split off coating material to be around 220 nm and 240 nm, respectively. In order to obtain a PB capacity (Q (mC cm^{-2}) = I (µA cm^{-2}) × t (s)) equivalent to that of the PEDOT film, different conditions were tested varying the current density and the time. Grains with a diameter of around 300 nm for the low deposition current (−10 µA cm^{-2}) (Fig. 2b) and a diameter of 150 nm for the higher deposition current (−40 µA cm^{-2}) were observed.

These differences in surface morphology come from the mechanism of nucleation-growth of the PB. In the latter case (fast deposition), the nucleation of PB particles is favoured because of the higher current density, leading to smaller particles. A higher deposition rate is preferred to obtain lower grain size, but the films with a lower deposition rate are smoother. It should be mentioned that the electrochemical and spectro-electrochemical properties of these different films were similar.

The Raman spectrum of a typical isp-PEDOT film is displayed in Fig. 3. The spectrum is in good agreement with

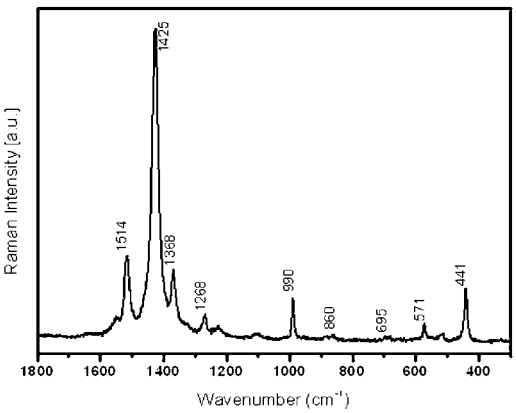

Fig. 3 Micro-Raman spectrum of isp-PEDOT in the oxidised state ($\lambda_{exc.} = 633$ nm).

the results reported by Tran-Van *et al.*[33] Accordingly, the band at 1514 cm^{-1} can be attributed to an asymmetric C=C stretching vibration of the thiophene rings in the middle of the polymer chains. The band at 1425 cm^{-1} is due to a symmetric Cα=Cβ stretching mode, while the emission at 1368 cm^{-1} is assigned to the Cβ–Cβ stretching deformation of the aromatic thiophene ring. The 1268 cm^{-1} band originates from an inter-ring Cα–Cα′ stretching mode and the undefined weak signal at 695 cm^{-1} is attributed to a C–S–C ring deformation. The following bands are assigned to oxyethylene ring modes: ring deformation at 990 cm^{-1}, O–C–C deformation at 860 cm^{-1}, and C–O–C deformations at 571 cm^{-1} and 441 cm^{-1}.

The variation of the visible range absorbance of the individual films was studied in an ionic liquid-based liquid electrolyte [0.03/0.97 LiTFSI/BMI-TFSI (molar ratio)] by applying a potential from −1.0 V to +1.0 V *vs.* Ag/AgCl and from −1.0 V to +0.5 V *vs.* Ag/AgCl for PEDOT and Prussian Blue, respectively (Fig. 4a and b). This ionic liquid-based liquid electrolyte is fully transparent in this region as mentioned earlier.[34]

For Prussian Blue, a completely colourless bleached state was observed (curve h in Fig. 4b), whereas PEDOT still showed a residual light blue colouration in the bleached state (curve k in Fig. 4a). The spectra show broad absorption bands centred at 720 nm and 610 nm for PB and PEDOT, respectively. Colouration efficiencies of 350 $cm^2\ C^{-1}$ (at 610 nm) and 78 $cm^2\ C^{-1}$ (at 720 nm) were determined for PEDOT and PB, respectively.

In order to build up charge balanced electrochromic devices, the capacities of the PB films were adapted to match those of the PEDOT films. The volta-absorptometry of isp-PEDOT in the ionic liquid electrolyte used in this study has already been published,[35] that of PB is illustrated in Fig. 5. The variation of absorbance at 720 nm for PB is clearly correlated to the cyclic voltammogram. In the 0.2 V to −1.0 V range, the negative value of dA/dt indicates the decrease in absorbance when the reduction of PB to the Fe^{II}–Fe^{II} form of Prussian White (PW) takes place. Subsequently, oxidation of PW to PB between

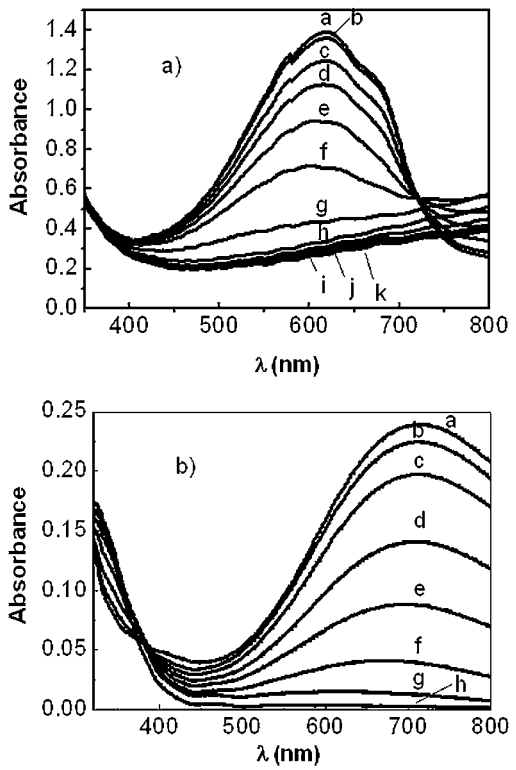

Fig. 4 Variation of the absorbance for different applied potentials (ref.: Ag/AgCl, counter electrode = Pt wire) of: (a) a PEDOT film [(a) −1.3 V, (b) −1 V, (c) −0.7 V, (d) −0.6 V, (e) −0.5 V, (f) −0.4 V, (g) −0.3 V, (h) −0.2 V, (i) 0 V, (j) 0.2 V, (k) 0.3 V] and (b) a Prussian Blue film: [(a) 0.5 V, (b) 0.3 V, (c) 0.2 V, (d) 0.1 V, (e) 0 V, (f) −0.1 V, (g) −0.2 V, (h) −1 V].

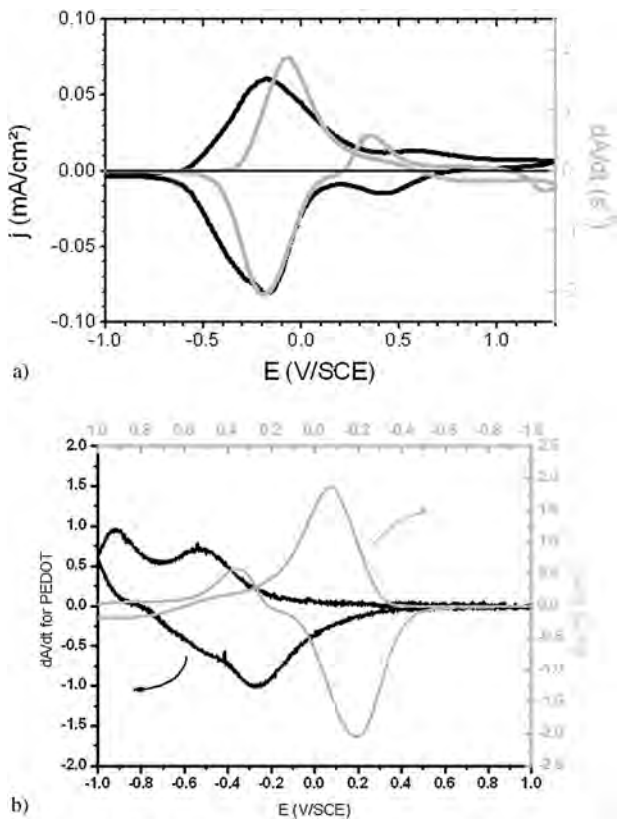

Fig. 5 (a) Cyclic voltammetry at 8.3 mV s^{-1}, $j = f(V)$ on the left axis and cyclic volta-absorptometry $dA/dt = f(V)$ at 720 nm on the right axis for Prussian Blue on TCO/glass; reference electrode SCE. (b) Volta-absorptometry of PEDOT and PB films.

−1.0 V and 0.2 V generates a positive dA/dt. The variation of dA/dt in the 0.5 V to 1.3 V range is presumably due to Berlin Green formation (slight overoxidation of PB).[36]

Volta-absorptometry was a powerful tool at this stage to determine the maximum variation in colouration at the smallest possible potential range. Indeed, in the case of PEDOT, in a certain range of potential (depending on the nature of the PEDOT), redox reactions have been shown to take place in the film without any conceivable visible colouration (absorption occurs in the NIR region).[35] For PB, such phenomenon was not observed, the colouration change being directly proportional to the number of produced 'blue' colour centres. Comparing the two films (Fig. 5b) helped determining the effective potential range for achieving a full colour change (−1.0 V to 0.5 V *vs.* SCE).

ECD study: influence of the TCO sheet resistance

A first experiment was performed to assess the influence of the transparent conductive oxide on the device performance. Devices were assembled using different 5 × 5 cm^2 sized (5 × 4 cm^2 active area) ITO/glass panels with sheet resistances of 24, 58, and 124 Ω sq^{-1}. The data were then compared to those obtained for a device based on ITO/PET flexible substrates with a sheet resistance of 60 Ω sq^{-1}. The device overall charge capacity (around 1.2 mC cm^{-2} for all samples) was measured by cyclic voltammetry[37] after cycle no. 1 and cycle no. 1000. A long term capacity loss of between 2 and 15% was apparent, presumably due to the absence of sealing/encapsulation measures (diffusion of moisture and air into the device).

The devices showed comparable response in cyclic voltammetry measurements (500 mV min^{-1}, −1.0 V to +1.0 V *vs.* RE). Absorption occurs between 500 nm and 900 nm covering a wide part of the visible spectrum. A blue transmitted colour resulted due to the added-up absorbance of PEDOT and PB. As a representative example, pictures of the bleached and coloured states as well as spectro-electrochemistry data [colouration efficiency (CE) and contrast ratio (CR = $T_{coloured}(\%)/T_{bleached}(\%)$)] of a complete device (configuration A, substrate sheet resistance: 24 Ω sq^{-1}) are presented in Fig. 6. CE is defined as the change in optical density (absorbance) (ΔA) per unit of an inserted charge and is calculated using the formula CE = $\Delta A/Q$.[3]

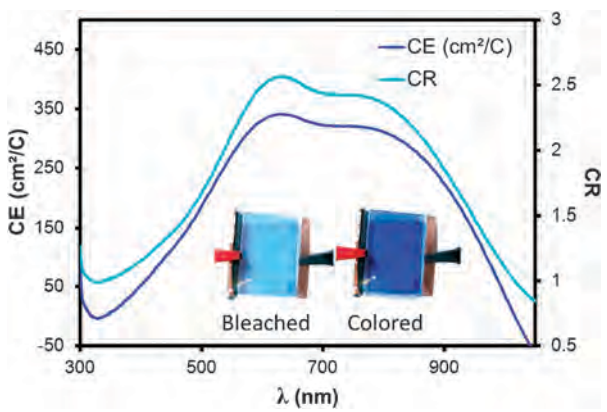

Fig. 6 Variation of the colouration efficiency (dark blue) and the contrast ratio (light blue) of a complete isp-PEDOT/PB device with the wavelength (configuration A with 24 Ω sq^{-1} ITO sheet resistance).

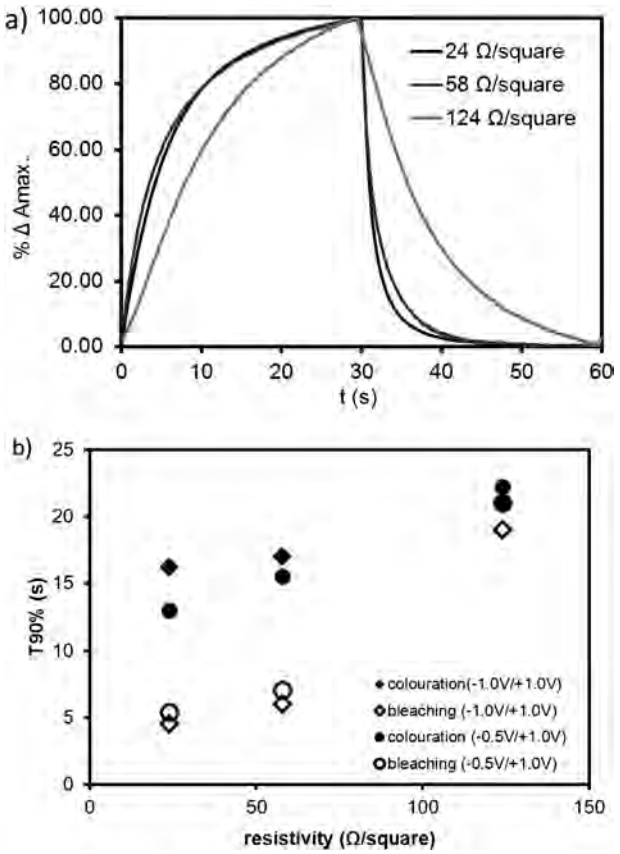

Fig. 7 (a) Kinetics of colouration and bleaching at 640 nm obtained by switching the potentials from −1 V to +1 V. (b) Variation of the response time $T_{90\%}$ depending on ITO sheet resistance for two different potential steps.

The residual colour in the bleached state is due to the well-known light blue oxidised state of PEDOT. High composite colouration efficiencies have been obtained for these devices with a maximum CE of 338 cm^2 C^{-1} at 640 nm.

The variation of the electrochromic response times $T_{90\%}$ with the sheet resistance is given in Fig. 7 for two voltage steps: −0.5 V–30 s/+1.0 V–30 s and −1.0 V–30 s/+1.0 V–30 s. $T_{90\%}$ is the time necessary to reach 90% of full colouration and bleaching.

The results depicted in Fig. 7 clearly show a correlation between the sheet resistance of the substrate and the switching kinetics.

The higher the resistance of the ITO layer (*i.e.* the lower the electrical conductivity), the slower the kinetics of the devices. This holds regardless of whether colouration or bleaching is considered.

Bleaching proved to be generally faster than colouring, which corresponds to the usual behaviour of PEDOT films. It is noteworthy that for 58 Ω sq^{-1} ITO, colouration and bleaching times were independent of the applied reduction potential (−0.5 V or −1.0 V).

ECD study: influence of the PMMA content in the gel electrolyte layer

The optimisation of the PMMA content in the electrolyte mixture is crucial in terms of mechanical and optical properties of the resulting layer. For a use in complete ECDs, the amount of PMMA has to be traded-off with parameters such as

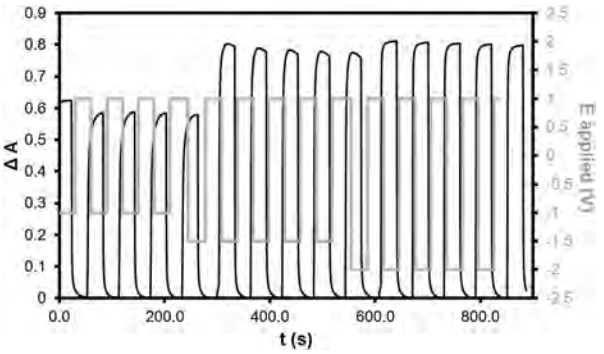

Fig. 8 Spectro-electrochemistry of a complete device assembled using a 70 wt% (0.03/0.97 LiTFSI/BMITFSI)–30% PMMA electrolyte mixture: variation of absorbance change.

stickiness, transparency, and mechanical stability. A highly conductive 10 Ω sq^{-1} FTO/glass electrode was used in a particular experiment in order to reduce the effect of substrate sheet resistance. Layers formed from 0.03/0.97 LiTFSI/BMI-TFSI mixtures (molar ratio) containing 30, 40, and 50 wt% of PMMA were placed in between the PEDOT and PB layers ($4 \times 5\ cm^2$ of active area). The spectro-electrochemical properties were determined by applying various fixed potentials during 30 s and measuring the change in absorbance (ΔA) of the complete device (Fig. 8) at 640 nm. Despite the slight residual colouration in the bleached state, the device showed a high ΔA (0.77) and a CE of 335 $cm^2\ C^{-1}$ for the 30 wt% variant.

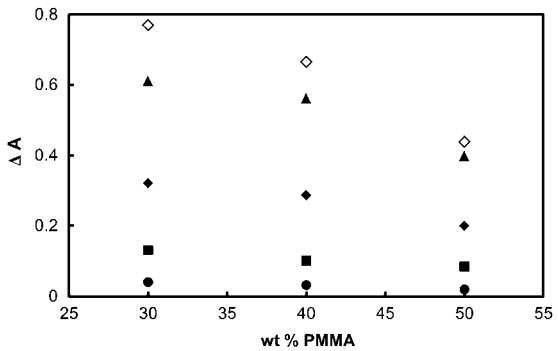

Fig. 9 Variation of the absorbance change (ΔA) between coloured and bleached states at 640 nm ($\Delta A = 0$ at $E = 1$ V) with different PMMA weight ratios at various applied potentials: (●) 0.5 V; (■) 0.0 V; (◆) −0.5 V; (▲) −1.0 V; (◊) −1.5 V.

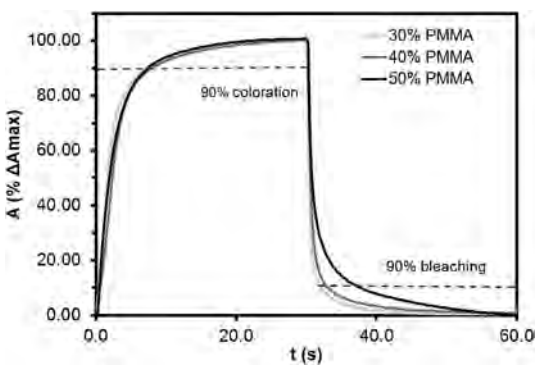

Fig. 10 Kinetics of colouration and bleaching at 640 nm between potentials of −1 V for colouring and +1 V for bleaching.

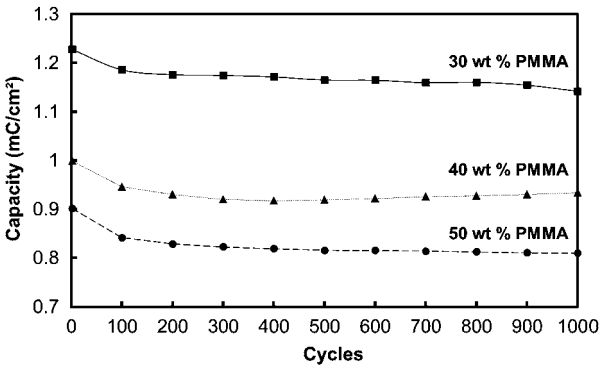

Fig. 11 Variation of the charge capacity during cycling between −1.0 V/5 s and +1.0 V/5 s of devices assembled with 30 to 50 wt% PMMA in 0.03 LiTFSI/0.97 BMI-TFSI electrolyte mixtures.

The variation of absorbance change (ΔA), the kinetics, and the cycling behaviour of devices employing electrolytes with PMMA contents ranging from 30 to 50 wt% are illustrated in Fig. 9–11.

The colouration kinetics defined by the time necessary to reach 90% of the maximum colouration (640 nm) was constant (7 s), regardless of the PMMA content. In contrast to that, the bleaching time significantly increased from 2 s for 30 wt% PMMA to 7 s for 50 wt% PMMA (Fig. 10).

Long term cycling was performed by means of chrono-amperometry (10 s) in the −1.0 V/+1.0 V range (Fig. 11). A delay of 10 s was chosen in order to ensure that the system reached equilibrium at 90% of its maximum contrast. After a first period of formatting over the first 200 cycles, the charge capacities became nearly constant (<3% decrease between 200 and 1000 cycles).

For all devices, a similar loss of around 15% was observed for the ΔA value after 1000 cycles. This result is considered very promising since no protective sealing was used at that stage. Moreover, after 4 months of storage time, the systems still exhibited very high electrochromic stability with a ΔA loss of less than 1%.

Therefore, ECDs of the described configurations are effective in terms of electrochromic performance and long-term stability, both under cycling (up to 1000 cycles) and at-rest (4 months) conditions. The parameter mostly impacted by cycling was found to be the change of absorbance ΔA.

ECD up-scaling

The incorporation of PMMA into the BMI-TFSI/LiTFSI electrolyte mixture yielded adhesive and semi-solid membranes having strong advantages: (i) they allow the preparation of leakage-free, moisture-free, and short circuit-free solid-state devices; (ii) their shape can be adapted to any kind of substrates including curved or flexible ones. As will be shown in the following, such membranes may also be used in plastic-based flexible electrochromic devices of larger size.

Prior to up-scaling, however, a test was performed with a $4 \times 5\ cm^2$ sized device using the ITO/PET film with a sheet resistance (60 Ω sq^{-1}) close to that of ITO/glass of medium resistance (58 Ω sq^{-1}). The system exhibited a charge capacity of 2.5 mC cm^{-2}, a colouration efficiency of 270 $cm^2\ C^{-1}$ (640 nm), and a contrast ratio of 4.7 after 10 min of formatting. Response times for colouration and bleaching were comparable

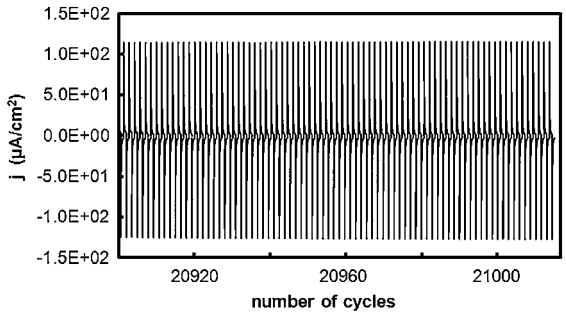

Fig. 12 Last chrono-amperometric cycles of a large device scanned between +1.0 V (90 s) and −1.5 V (90 s).

to those obtained when the ITO/glass was used as substrate (12 and 6 s, respectively). This latter result suggests that ECDs built up on the ITO/PET film may exhibit similar properties as ITO/glass-based EC elements, provided the sheet resistance is equivalent. Consequently, the chemical nature of the substrate (PET or glass) is believed to be of minor importance for the electrochromic response, the sheet resistance value being the only crucial parameter.

The benchmark system described above was scaled up to a size of 12 × 15 cm^2 (active area). The bleached and darkened states were of transparent sky blue and deep blue colour, respectively. The device was sealed on the edges with a resilient scotch tape and cycled over more than 21 000 cycles (average capacity of 1.4 mC cm^{-2}) to check the long-term stability when going to larger sizes. Apparent defects were few in numbers and could be attributed to the manual handling and set-up. The study revealed a continuously high homogeneity and long-term cycle life (see stable chrono-amperometry during the last cycles in Fig. 12) corresponding to a durability of 6 years when 10 switching cycles per day are assumed.

The electrochromic properties of the device (Fig. 13 and 14) were determined after 10, 450, and 21 000 cycles. The levels of transmittance were unchanged after 450 cycles both in the

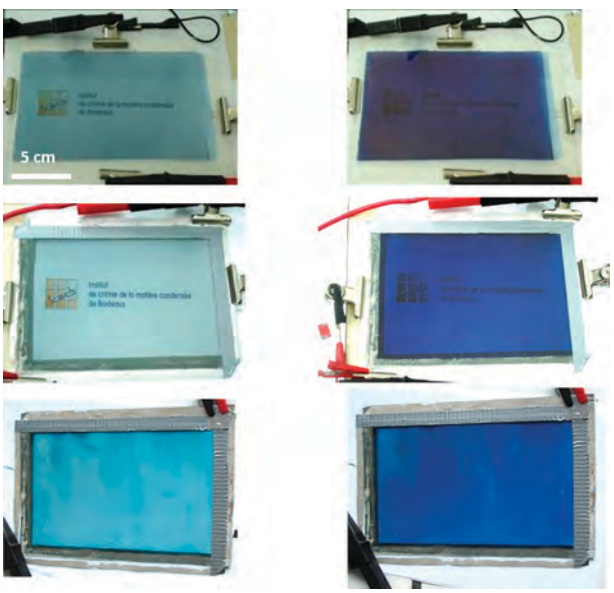

Fig. 13 Bleached and fully coloured states of the scaled-up device, after 10, 450, and 21 000 cycles (from top to bottom, respectively).

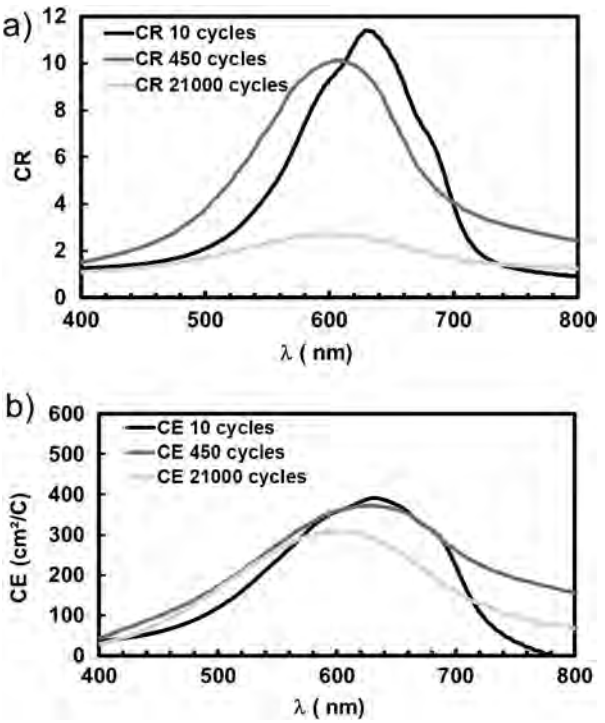

Fig. 14 Contrast ratio and colouration efficiency of the scaled-up device in the 400–800 nm range after 10, 450, and 21 000 cycles.

coloured and bleached states (Fig. S1, ESI‡). A significant decay of the contrast ratio was, however, observed after 21 000 cycles (Fig. 14a). The colouration efficiency (Fig. 14b), being an intrinsic material property, should be unchanged, unless material degradation occurs. Its slight decrease with the number of cycles suggests that indeed electrochemical side reactions might have taken place with time, consuming current without giving any colouration. This result highlights the necessity of a more effective sealing when it comes to achieving ultimate durability.

It is noteworthy that the devices showed reasonable performance, even though they were prepared manually and with sub-optimal sealing. Industrial manufacturing of electrochromic films, gel electrolyte membranes, and the full device (for example by roll-to-roll coating and lamination) is believed to lower the quantity of defaults and increase the device lifetime. In addition, the employment of industrial encapsulation processes (*e.g.*, moisture barrier layers, special edge sealing) is expected to result in further durability improvement. After all, the electrochromic properties of the system described above compare advantageously with published results as illustrated in Table 1.

Conclusions

Complete glass- and plastic-based electrochromic devices were prepared (i) to validate the use of ionic liquid based gel electrolyte membranes, (ii) to get a more accurate estimation of how different parameters can influence the device properties. Two factors were of particular interest, namely the PMMA content in the electrolyte and the TCO sheet resistance. It was shown that increasing the PMMA content (from 30 to 50 wt%) mainly caused a decrease in ΔA, *i.e.*, the change in absorbance

Table 1 Electrochromic performance of different PEDOT/PB devices

Electrochromic layer	Electrolyte	Electrode (area/cm^2)	CE/cm^2 C^{-1} (λ/nm)	Ref.
PEDOT doped with Viologen/PB	$LiClO_4$/PC	PEDOTPSS/PET (-)	187 (693)	38
PEDOT/PB	AN/PC/PMMA/Li[$N(SO_2CF_3)_2$] (70 : 20 : 7 : 3)	ITO/Glass (2 × 2)	338 (590)	39
PEDOT/PB	PVA/NH_4SCN/DMSO	FTO/Glass (5 × 5)	120 (595)	40
PEDOT/PB	PVA/BMePyTfI/DMSO[a]	FTO/Glass (4 × 3)	274 (602)	41
In-situ PEDOT	LiTFSI/BMI-TFSI/PMMA	ITO/PET (12 × 15)	310 (600)[b]	This work

[a] Polyvinyl alcohol: PVA, BMePyTfI: (1-butyl-1-ethylpyrrolidinium-bis(trifluoromethyl sulfonyl)imide. [b] After 21 000 cycles.

during the electrochromic switching process. On the other hand, an increase in TCO sheet resistance resulted in slower switching kinetics. Changes from 4 to 19 s and from 16 to 21 s were observed for bleaching and colouration, respectively. While the sheet resistance of the TCO strongly affected the response times, the nature of the substrate did not.

The devices showed a noticeable performance decrease upon long-term cycling. However, their properties nevertheless are rated promising considering that a manual assembly of laboratory scale devices was performed. Manufacture on an industrial scale is believed to result in substantial improvement of quality of the films, of the interface between the layers, and of the sealing, all of which will ensure a much better lifetime. As compared to earlier reports on PEDOT-based devices, the transmittance of the bleached state and hence the optical contrast have been improved due to the use of moderator-controlled *in situ* chemical oxidative polymerisation.

Acknowledgements

The research leading to these results has received funding from the European Union's Sixth and Seventh Framework Programmes under grant agreements no. 505664 and no. 200431, respectively. Contribution from the CNRS *via* the "Programme Interdisciplinaire Energie": NANODISFLEX is also acknowledged.

Notes and references

1 S. Sadki, P. Schottland, N. Brodie and G. Sabouraud, *Chem. Soc. Rev.*, 2000, **29**, 283.
2 G. A. Niklasson and C. G. Granqvist, *J. Mater. Chem.*, 2007, **17**, 127.
3 C. G. Granqvist, *Handbook of Inorganic Electrochromic Materials*, Elsevier, Amsterdam, 1995.
4 H. J. Byker, *Electrochim. Acta*, 2001, **46**, 2015.
5 F. Dogan, H. Hadavinia, S. J. Bartonand and P. J. Mason, *Recent Pat. Mech. Eng.*, 2010, **3**, 174.
6 P. A. Kilmartin and J. Travas-Sejdic, *Nanostructured Conducting Polymers*, ed. A. Eftekhari, John Wiley & Sons Ltd, Chichester, UK, 2010, ch. 15, p. 599.
7 J. Huang and Z. Wie, *Nanostructured Conducting Polymers*, ed. A. Eftekhari, John Wiley & Sons Ltd, Chichester, UK, 2010, ch. 11, p. 467.
8 R. Ravichandran, S. Sundarrajan, J. R. Venugopal, S. Mukherjee and S. Ramakrishna, *J. R. Soc. Interface*, 2010, **7**, S559.
9 D. R. Rosseinsky and R. J. Mortimer, *Adv. Mater.*, 2001, **13**, 783.
10 R. D. Rauh, *Electrochim. Acta*, 1999, **44**, 3165.
11 S. Kirchmeyer, A. Elschner, K. Reuter, W. Lovenich and U. Merker, *PEDOT as a Conductive Polymer: Principles and Applications*, CRC Press Inc, 2010, ch. 8.
12 S. I. Cho and S. B. Lee, *Acc. Chem. Res.*, 2008, **41**, 699.
13 D. Melepurath, A. Arvind and B. Shweta, *Phys. Chem. Chem. Phys.*, 2009, **11**, 5674.
14 N. Rozlosnik, *Anal. Bioanal. Chem.*, 2009, **395**, 637.
15 Y. Yoshioka and G. E. Jabbour, *Inkjet Printing and Patterning of PEDOT-PSS Application to Optoelectronic Devices*, *Handbook of Conducting Polymer: Conjugated Polymers, Processing and Applications*, CRC Press, 3rd edn, 2007, ch. 3.
16 C. Winder and N. S. Sariciftci, *J. Mater. Chem.*, 2004, **14**, 1077.
17 H. W. Heuer, R. Wehrmann and S. Kirchmeyer, *Adv. Funct. Mater.*, 2002, **12**, 89.
18 S. Bhandari, M. Deepa, A. K. Srivastava, S. T. Lakshmikumar and R. Kant, *J. Nanosci. Nanotechnol.*, 2009, **9**, 3052.
19 D. C. Martin, J. Wu, C. M. Shaw, Z. King, S. A. Spanninga, S. Richardson-Burns, J. Hendricks and J. Yang, *Polym. Rev.*, 2010, **50**, 340–384.
20 K. E. Aasmundtveit, E. J. Samuelsen, L. A. A. Pettersson, O. Inganäs, T. Johansson and R. Feidenhans, *Synth. Met.*, 1999, **101**, 561.
21 Y. T. Kim, C. M. Park, E. J. Kim and K. S. Suh, *Synth. Met.*, 2005, **149**, 169.
22 A. Lima, P. Schottland, S. Sadki and C. Chevrot, *Synth. Met.*, 1998, **93**, 33.
23 US Patent 2004/0085711A1/EP 1391 474 (Bayer Corp.).
24 V. D. Neff, *J. Electrochem. Soc.*, 1978, **125**, 886.
25 K. Itaya, T. Ataka and S. Toshima, *J. Am. Chem. Soc.*, 1982, **104**, 4767.
26 S. Duluard, J. Grondin, J.-L. Bruneel, G. Campet, M.-H. Delville and J.-C. Lassègues, *J. Raman Spectrosc.*, 2008, **39**, 1189.
27 M. P. Scott, C. S. Brazel, M. G. Benton, J. W. Mays, J. D. Holbrey and R. D. Rogers, *Chem. Commun.*, 2002, 1370.
28 *Polymer Handbook*, ed. J. Brandrup, E. H. Immergut, E. A. Grulke, A. Abe and D. R. Bloch, John Wiley & Sons, © 1999, 4th edn, 2005.
29 G. Campet, C. Mingotaud, J.-N. Portier and S. Ravaine, *patent no. WO0152338*, 2001.
30 M. Deepa, N. Sharma, S. A. Agnihotry, S. Singh, T. Lal and R. Chandra, *Solid State Ionics*, 2002, **152–153**, 253.
31 Y. Ha, N. Nikolov, S. Pollack, J. Mastrangelo, B. Martin and R. Shashidhar, *Adv. Funct. Mater.*, 2004, **14**, 615.
32 R. Ruffo, A. Celik-Cochet, U. Posset, C.-M. Mari and G. Schottner, *Solar Energy Mater. Solar Cells*, 2008, **92**, 140.
33 F. Tran-Van, S. Garreau, G. Louarn, G. Froyer and C. Chevrot, *J. Mater. Chem.*, 2001, **11**, 1378.
34 S. Duluard, I. Litas, A. J. Bhattacharyya, F. Mauvy, G. Campet and M.-H. Delville, *Electrochim. Acta*, 2010, **55**, 8839.
35 S. Duluard, B. Ouvrard, A. Celik-Cochet, G. Campet, U. Posset, G. Schottner and M.-H. Delville, *J. Phys. Chem. B*, 2010, **114**, 7445.
36 P. J. Kulesza, S. Zamponi, M. A. Malik, K. Miecznikowski, M. Berrettoni and R. Marassi, *J. Solid State Electrochem.*, 1997, **1**, 88.
37 *Applications of Electroactive Polymers*, ed. B. Scrosati, Chapman & Hall, London, 1993.
38 S. Bhandari, M. Deepa, S. Pahal, A. G. Joshi, A. K. Srivastava and R. Kant, *ChemSusChem*, 2010, **3**, 97.
39 T.-S. Tunga and K.-Ch. Ho, *Solar Energy Mater. Solar Cells*, 2006, **90**, 521.
40 M. Deepa, A. Awadhia, S. Bhandari and S. L. Agrawal, *Electrochim. Acta*, 2008, **53**, 7266.
41 M. Deepa, A. Awadhia and S. Bhandari, *Phys. Chem. Chem. Phys.*, 2009, **11**, 5674.